A New Identification Method of Underground Excavation Based on Velocity Estimation Using Double Point Synchronous Measurements

DONGZE QIN[1], AND JINSHI ZHANG[1,2]

[1]School of Mechatronic Engineering, North University of China, Taiyuan 030051, China
[2]Advanced Manufacturing Technology Laboratory in Shanxi, North University of China, Taiyuan 030051, China

Corresponding author: Dongze Qin (apo1981@126.com)

ABSTRACT In an assault on a military fortress, the attacking side often attacks the fortress through the use of underground mining, so that the defensive side cannot be prepared. The existing monitoring methods make it difficult to monitor such underground excavation. One effective way to monitor for tunneling activity is to detect and identify seismic signals generated by underground excavation. However, the main problem facing the practical application of this technology is that many behaviors on the ground may generate seismic signals, and the monitoring system cannot identify whether a signal is generated by underground excavation or by someone walking on the ground, resulting in a high false alarm rate. To effectively identify underground excavation signals, we propose an approach for estimating speed based on a double point synchronization measurement. In our approach, we first formulate mathematical models of the velocities of underground and ground-level objects. Then, signals acquired by different seismic detectors are used to estimate the velocities of underground and ground-level objects. By analyzing the differences between velocities, signals due to human movement and underground excavation are effectively identified. Lastly, simulations and a field test are performed. It is found that the proposed approach can effectively distinguish between signals generated by a human moving at ground-level and underground excavation. Our approach can be helpful for reducing the false alarm rate of a monitoring system.

INDEX TERMS Identification method, underground excavation, velocity estimation, measurements.

I. INTRODUCTION
A. BACKGROUND

At present, there are several major types of equipment and preventive measures used in the fields of military fortification and security monitoring, including infrared detection, video monitoring, microwave detection, acoustic detection, ultrasonic detection, vibration detection, and so on. These devices have important roles in preventing crime and providing early warnings. However, for new methods of crime, such as stealing by digging a tunnel, the effectiveness of these techniques is minimal. Moreover, this type of crime not only appears in the banking, treasury and other civil fields but also impacts areas like prisons and national borders.

The necessity of discovering these criminal behaviors, including illegal entry into another country, the invasion of a bank's vault, escape from prison, etc., committed using underground excavation, highlights the need for new security monitoring technologies.

The current monitoring method is image monitoring, and the literature presents an interactive security monitoring system based on passive infrared motion detection sensors, which capture images of any intruding persons and provide them to everyone using the system, both on an Android platform and in an online portal [1]. There has been less research on ground vibration monitoring in underground excavation. Most studies have examined transverse and longitudinal waves in strong earthquakes, such as the use of a small reflector for monitoring ground motion in SAR [2]. Some scholars have studied anti-interference and new methods for detecting

---

The associate editor coordinating the review of this manuscript and approving it for publication was Jenny Mahoney.

traveling wave signals [3]. Some authors use rotation and translation ground motion sensors at the same location to characterize the seismic scattering in a P-wave wake [4]. The mixed anfis-pso model has also been used to predict over break in underground caverns [5]. In addition, some studies have been based on parameter sensitivity analysis of the influence of underground excavation on slope stability by the vector sum method [6]. Experimental data on the stress state of salt rock in an underground cavern have been reported [7].

In this paper, shallow excavation is studied. The main application is shallow ground to indicate the propagation of Rayleigh waves. The propagation characteristics of the shear wave, longitudinal wave and Rayleigh wave are different.

For underground excavation monitoring, the literature is primarily focused on the application of monitoring combined with numerical analysis in the safe excavation of large-scale hydropower underground complexes. The literature discusses the fact that these 3D analyses simulate step-by-step excavation while predicting the stress-strain behavior [8]. The literature investigates an approach to seismic pattern recognition comprising wavelet-based feature extraction, feature selection based on mutual information criteria, and neural classification based on feed-forward networks [9].

At present, there is very little literature directly related to the monitoring of underground excavation. There are many studies on the recognition of people and vehicles on the ground based on seismic information from a ground sensor network system [10]–[13]. Advanced and complex signal methods are often used to process ground motion information, but the calculation amount is relatively large because machine-aided learning is required [14], [15].

The environment of an underground excavation monitoring system is complex. Generally, the speed of underground excavation is slow and is closest to the walking speed of people. Other types of interference, such as driving of vehicles, and the natural environment, such as wind or rain, differ greatly from underground excavation in terms of speed. Personnel are likely to walk within the monitoring area. If the activity caused by personnel walking within the monitoring area is detected as digging behavior, then a false alarm will result. Moreover, if a person walks in the monitoring area while underground excavation is taking place, the system may determine that a person is simply walking in the monitoring area, which could cause a missed alarm [16], [17].

For ground target recognition, the traditional research method is to use advanced signal processing algorithms for pattern recognition. Based on data and experiments, the present study finds that the most remarkable feature of underground mining is the slow speed of mining (compared with the ground target), which is usually implemented manually and limited by the geographical environment. In view of this characteristic, modeling, simulation and experimental research were performed, and the results revealed that the method mentioned in this paper is feasible.

B. WORK AND CONTRIBUTION

(1) We propose a method for estimating speed based on a two-point synchronization measurement. Seismic signals are synchronously obtained by two seismic detectors, and the target speed is estimated. By applying the estimated target speed and combining the speed difference between the ground-level walking speed and the underground mining speed, an underground excavation can be effectively identified.

(2) We analyze the formation and propagation principle of seismic signals. Then, we estimate and predict a model for the velocities of objects, including the expected value, variance and confidence interval, and calculate and simulate these values. By analyzing the simulation results, it is shown that the errors of the statistical velocities are within the acceptable range of an underground excavating system.

(3) We develop seismic detectors that meet the relevant technical requirements. Furthermore, we implement experiments using two seismic detectors. The experimental results show that there exist great differences between the velocities of signals generated by underground excavation and ground-level human movement. The feasibility of the proposed approach for recognizing underground signals using their velocity features is also verified.

II. MATHEMATICAL MODELING
A. FORMATION AND PROPAGATION PRINCIPLE OF GROUND MOTION SIGNALS

Underground excavation and ground targets will stimulate the ground during movement, causing deformation of the surface medium, which can be propagated in the medium to form seismic waves. The most common waves in seismic wave detection are longitudinal waves, transverse waves, and Rayleigh waves. Among these, the longitudinal wave, which is the highest frequency wave, travels the fastest, while the transverse wave, with less energy, goes slower. The Rayleigh wave, which spreads along the free surface, is lower in frequency, has the highest energy, and has the longest transmission distance. A large number of experiments have shown that seismic waves are primarily composed of Rayleigh waves. Therefore, Rayleigh waves are widely used in seismic signal analysis [18]–[20].

B. TARGET VELOCITY INFORMATION MODELING

For convenience, the people excavating underground and the people walking at ground level are collectively referred to as the target; the underground excavation and personnel walking speed information are collectively referred to as the target speed information. Because the speed of the underground excavation and that of the personnel walking at ground level are quite different, we can use two ground motion detectors to obtain monitoring information for calculating the target speed and then determine whether the detected target corresponds to underground excavation based on the target speed. The calculation of the target velocity depends on four observations from two adjacent seismic detectors, shown as S_1 and S_2
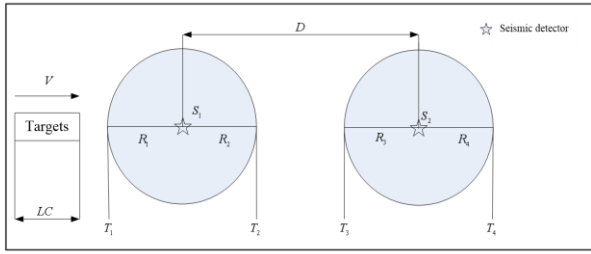
FIGURE 1. Two adjacent seismic detectors.

shown in Fig.1. Each seismic detector records the moment when it first detects the target and the time at which the target leaves its detection range.

D – The linear distance between two adjacent ground motion detectors

T_m – The time in which the target passes two adjacent ground motion detectors

T_1 – The starting time of the target detected by S_1

T_2 – The departure time of the target detected by S_1

T_3 – The starting time of the target detected by S_2

T_4 – The departure time of the target detected by S_2

R_1 – The detection radius of S_1 near the target side

R_2 – The detection radius of S_1 far from the target side

R_3 – The detection radius of S_2 near the target side

R_4 – The detection radius of S_2 far from the target side

V – The average speed of the target

$\hat{V}$ – The estimated speed of the target

The estimation of target speed involves the distance and time interval between the two seismic detectors. The calculation method of the estimated speed determined by the seismic detector is given in formula (1).

$$\hat{V} = \frac{D}{T_m} \qquad (1)$$

1. Basic assumptions $\hat{V}$

(i) The distance between the two seismic detectors is known when the detector of the underground excavation monitoring system is laid.

(ii) The target moves at an average speed of V in a straight line.

(iii) The detector is placed in an area with a homogenous soil type. The detection area of the sensor is circular, and the sensor is placed in the center of the area. In practice, because the position of the ground motion detector after installation is fixed, the error caused by soil inhomogeneities can be overcome by increasing the correction coefficient. Therefore, it is assumed that the consistency of soil properties will not have a significant impact on the engineering of this method.

(iiii) No other interference (such as wind, rain, driving vehicles, etc.).

2. The estimation model of target velocity

T_m is the time in which the target passes the two adjacent ground motion detectors. The calculation is shown in equation (2).

$$T_m = \left[T_3 + \left(\frac{T_4 - T_3}{2} \right) \right] - \left[T_1 + \left(\frac{T_2 - T_1}{2} \right) \right] \qquad (2)$$

The time is measured in minutes. The detection cycle begins when the target is detected by the seismic detectors for the first time, designated as T_1, which serves as the baseline time during the whole process of monitoring. Based on the relationship between time, distance and speed, we can define other times by using formula (3).

$$T_2 = T_1 + \frac{R_1 + R_2 + LC}{V} \qquad (3)$$

$$T_3 = T_1 + \frac{R_1 + D - R_3}{V}. \qquad (4)$$

$$T_4 = T_1 + \frac{R_1 + D + R_4 + LC}{V} \qquad (5)$$

T_m can also be expressed as a function of R, which is derived as follows.

$$
\begin{aligned}
T_m &= \left[T_3 + \left(\frac{T_4 - T_3}{2} \right) \right] - \left[T_1 + \left(\frac{T_2 - T_1}{2} \right) \right] \\
&= \frac{T_4 + T_3 - T_2 - T_1}{2} \\
&= \frac{1}{2} \left[\left(T_1 + \frac{R_1 + D + R_4 + LC}{V} \right) \right. \\
&\quad + \left(T_1 + \frac{R_1 + D - R_3}{V} \right) - \left(T_1 + \frac{R_1 + R_2 + LC}{V} \right) - (T_1) \right] \\
&= \frac{R_1 - R_2 - R_3 + R_4 + 2D}{2V} \qquad (6)
\end{aligned}
$$

Formula (6) is the basis of the estimation $\hat{V}$.

3. The statistical model of target velocity

Assuming that R_j is constant and independent of the distribution of random variables regardless of the distance from a given vibration detector, the distribution of R corresponding to S_1 and the distribution of R corresponding to S_2 are independent. The target speed V can be estimated by

$$E[T_m] = \frac{D}{V} \qquad (7)$$

σ_k^2 is the variance of R with respect to S_k, as described in formula (8).

$$Var(T_m) = \frac{\sigma_1^2 + \sigma_2^2}{2V^2} \qquad (8)$$

(i) $\hat{V}$ represents the second-order Taylor expansion of μ_{T_m}.

$$\hat{V} \approx \frac{D}{\mu_{T_m}} - \left(\frac{D}{\mu_{T_m}^2} \right) (T_m - \mu_{T_m}) + \frac{1}{2} \left(\frac{2D}{\mu_{T_m}^3} \right) (T_m - \mu_{T_m})^2 \qquad (9)$$

μ_{T_m} – The time in which the target passes two adjacent ground motion detectors (variable of a function).

In order to solve the problem more accurately, the second-order Taylor expansion value is used. From another point of view, the variance is only used as an auxiliary index, and

the first-order expansion is used to reduce the complexity of calculation on the basis of not affecting the research results.

Because $E\left[\left(T_m - \mu_{T_m}\right)\right] = 0$ the expected value can be expressed as formula (10).

$$
\begin{aligned}
E\left[\hat{V}\right] &\approx \frac{D}{\mu_{T_m}} + \frac{D}{\mu_{T_m}^3}\sigma_{T_m}^2 \\
&= \frac{D}{\left(\frac{D}{V}\right)} + \frac{1}{\left(\frac{D}{V}\right)^3}\left(\frac{\sigma_1^2 + \sigma_2^2}{2V^2}\right) \\
&= V\left(1 + \frac{\sigma_1^2 + \sigma_2^2}{2D^2}\right)
\end{aligned}
\tag{10}
$$

Formula (10) shows that the estimate $\hat{V}$ is too large. The deviation can be controlled by selecting the sensitivity of the ground vibration detector and increasing the distance between the detectors. The parameters of the combined seismic detector can be calculated from σ_c^2, and the unbiased estimate of velocity V is recorded as $\overset{\wedge}{V'}$. $\overset{\wedge}{V'}$ can be estimated by

$$
\overset{\wedge}{V'} = \left(\frac{D}{T_m}\right)\left(1 + \sigma_c^2\right)^{-1}
\tag{11}
$$

(ii) $\hat{V}$ is the first-order Taylor expansion of μ_{Tm}.

$$
\hat{V} \approx \frac{D}{\mu_{T_m}} - \frac{D}{\mu_{T_m}^2}\left(T_m - \mu_{T_m}\right)
\tag{12}
$$

Using the deviation correction factor in formulas (11) and (12), the corrected variance is formula (13).

$$
\begin{aligned}
Var\left(\overset{\wedge}{V'}\right) &\approx \left(1 + \sigma_c^2\right)^{-2}\sigma_{Tm}^2\left(\frac{D^2}{\mu_{Tm}^4}\right) \\
&= \left(1 + \sigma_c^2\right)^{-2}\left(\frac{\sigma_1^2 + \sigma_2^2}{2V^2}\right)\left(\frac{D^2}{\left(\frac{D}{v}\right)^4}\right) \\
&= V^2\sigma_c^2\left(1 + \sigma_c^2\right)^{-2}
\end{aligned}
\tag{13}
$$

(iii) For any given V, because the distribution R is unknown, the Chebyshev inequality is used to set the optimal boundary of the velocity estimate.

$$
P_r\left(\left|\overset{\wedge}{V'} - \mu_{\overset{\wedge}{V'}}\right| \leq t\right) \geq 1 - \frac{\sigma_{\overset{\wedge}{V'}}^2}{t^2} \approx 1 - \alpha
\tag{14}
$$

This formula allows a confidence interval of 2t for the expected probability. We can obtain a confidence interval of $(1 - \alpha)100\%$ for $\hat{V}$ by applying formula (14), and $\overset{\wedge}{V'}$ is computed by following the reduction.

$$
\begin{aligned}
&P_r\left(\left|\overset{\wedge}{V'} - \mu_{\overset{\wedge}{V'}}\right| \leq t\right) \\
&\geq 1 - \frac{\sigma_{\overset{\wedge}{V'}}^2}{t^2} \approx 1 - \alpha \\
&\Rightarrow P_r\left(\left|\overset{\wedge}{V'} - V\right| \leq t\right) \geq 1 - \frac{\sigma_{\overset{\wedge}{V'}}^2}{t^2} \approx 1 - \alpha
\end{aligned}
\tag{15}
$$

Using $\mu_{\overset{\wedge}{V'}} = V$, the inequality can be deduced as follows.

$$
\begin{aligned}
&t = \frac{\sigma_{\overset{\wedge}{V'}}}{\sqrt{\alpha}} \\
&\Rightarrow P_r\left(\left|\overset{\wedge}{V'} - V\right| \leq \frac{\sigma_{\overset{\wedge}{V'}}}{\sqrt{\alpha}}\right) \geq 1 - \alpha
\end{aligned}
\tag{16}
$$

Then, the upper and lower bounds of the target speed confidence interval can be deduced by using formula (16), where the upper bound is formula (17).

$$
\begin{aligned}
&V - \overset{\wedge}{V'} \leq \frac{V\sigma_c\left(1 + \sigma_c^2\right)^{-1}}{\sqrt{\alpha}} \\
&\Rightarrow V - \frac{V\sigma_c\left(1 + \sigma_c^2\right)^{-1}}{\sqrt{\alpha}} \leq \overset{\wedge}{V'} \\
&\Rightarrow V < \frac{\overset{\wedge}{V'}}{\left(1 - \frac{\sigma_c\left(1 + \sigma_c^2\right)^{-1}}{\sqrt{\alpha}}\right)}
\end{aligned}
\tag{17}
$$

The lower bound of the confidence interval is formula (18).

$$
V > \frac{\overset{\wedge}{V'}}{\left(1 + \frac{\sigma_c\left(1 + \sigma_c^2\right)^{-1}}{\sqrt{\alpha}}\right)}
\tag{18}
$$

III. SIMULATION AND EXPERIMENTAL ANALYSIS
A. SIMULATION ANALYSIS
This simulation analyzes the accuracy of the statistical model and the influence of the distance between the two seismic detectors on the accuracy. The range of a normal human's walking speed is 1.2m/s to 1.6m/s. According to engineering practice, the detection radius of the seismic detector can vary from 9m to 10m. For the tests, the distance between the two seismic detectors has been set for three different scenarios, with distances of 5m, 10m, and 15 m. The simulation is illustrated in Figures 2-4, and the data are shown in Table 1.
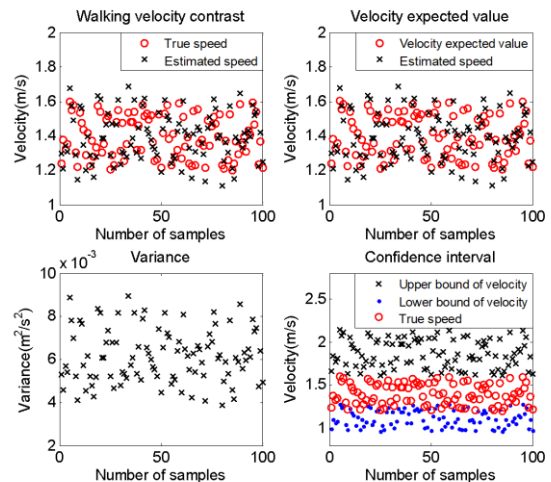

FIGURE 2. Walking simulation results (D=5 m).

TABLE 1. Simulation data statistics of walking.

D (m) (The distance between two detectors)	Walking velocity contrast (m/s)				Velocity expected value (m/s)				Variance (m²/s²)		Confidence interval (m/s)	
	Absolute deviation		Relative deviation		Absolute deviation		Relative deviation		Var (min)	Var(max)	V(min)	V(max)
	min	max	min	max	min	max	min	max				
5	0.0011	0.18	0.071%	13.98%	0.0019	0.18	0.12%	13.62%	0.0039	0.0090	0.97	1.61
10	5.51e-4	0.12	0.042%	7.74%	7.23e-4	0.12	0.047%	7.66%	0.0010	0.0022	1.08	1.82
15	5.10e-4	0.057	0.034%	4.04%	7.53e-6	0.058	0.0050%	4.07%	0.00050	0.00090	1.11	1.75

TABLE 2. Simulation data statistics of underground excavation.

D (m) (The distance between two detectors)	Excavation velocity contrast (m/s)				Velocity expected value (m/s)				Variance (m²/s²)		Confidence interval (m/s)	
	Absolute deviation		Relative deviation		Absolute deviation		Relative deviation		Var(min)	Var(max)	V(min)	V(max)
	min	max	min	max	min	max	min	max				
5	3.16e-5	0.021	0.075%	16.30%	2.09e-5	0.021	0.015%	15.9%	3.35e-7	0.00015	0.0087	0.27
10	1.55e-5	0.0089	0.028%	7.00%	3.94e-5	0.0090	0.026%	7.10%	1.09e-7	3.20e-5	0.01	0.23
15	2.60e-5	0.0056	0.020%	4.12%	3.30e-5	0.0056	0.060%	4.08%	6.83e-7	0.00020	0.010	0.22

FIGURE 3. Walking simulation results (D=10 m).
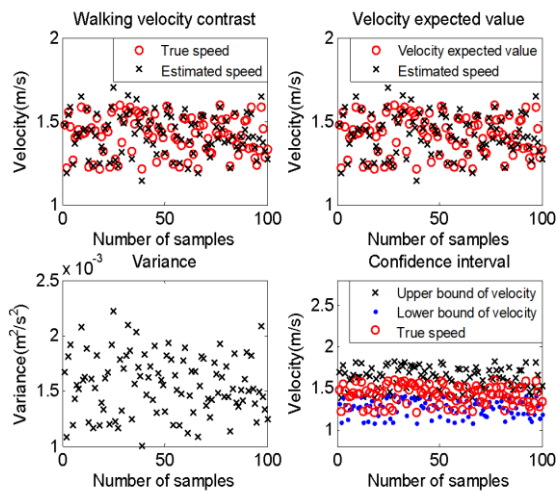

FIGURE 4. Walking simulation results (D=15 m).

The plots shown in Figures 2-4 reveal that the difference between the true value and the estimated value is not large. Table 1 lists the statistics of the data range in Figures 2-4. As shown in Table 1, when the distance between the two ground motion detectors is 5m, the relative deviation range for the walking speed and the mathematical model for the velocity estimation is (0.071%∼13.98%). The relative deviation of the estimated velocity and velocity expectation is (0.12%∼13.62%). The range of variance is (00039∼0.0090). When the confidence interval is 95%, the optimal boundary of the velocity estimate is (0.97m/s∼1.61m/s), and the estimated speed range is (1.11 m/s∼1.69 m/s).

When the distance between the two ground motion detectors is 10m, the relative deviation range of the walking speed and the mathematical model for the velocity estimation is (0.042%∼7.74%). T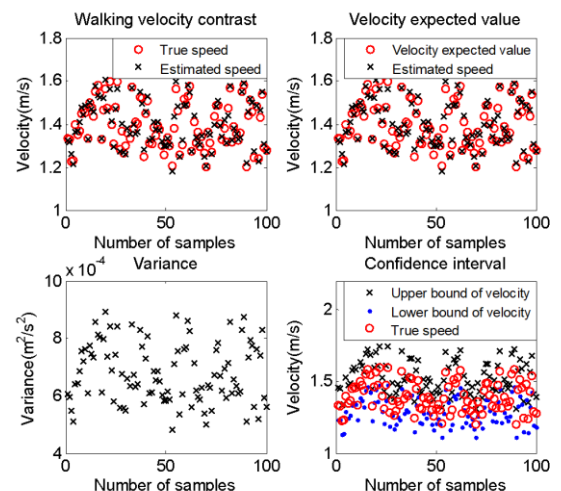he relative deviation of the estimated velocity and velocity expectation is (0.047%∼7.66%). The range of variance is (0.0010∼0.0022). When the confidence interval is 95%, the optimal boundary of the velocity estimate is (1.08 m/s∼1.82 m/s), and the estimated speed range is (1.14 m/s∼1.70 m/s).

When the distance between the two ground motion detectors is 15m, the relative deviation range of the walking speed and the mathematical model for velocity estimation is (0.034%∼4.04%). The relative deviation of the estimated velocity and velocity expectation is (0.0050%∼4.07%). The range of variance is (0.00050∼0.00090). When the confidence interval is 95%, the optimal boundary of the velocity estimate is (1.10m/s ∼1.75m/s), and the estimated speed range is (1.20 m/s ∼1.71 m/s).

The plots shown in Figures 5-7 show that the difference between the true value and the estimated value is
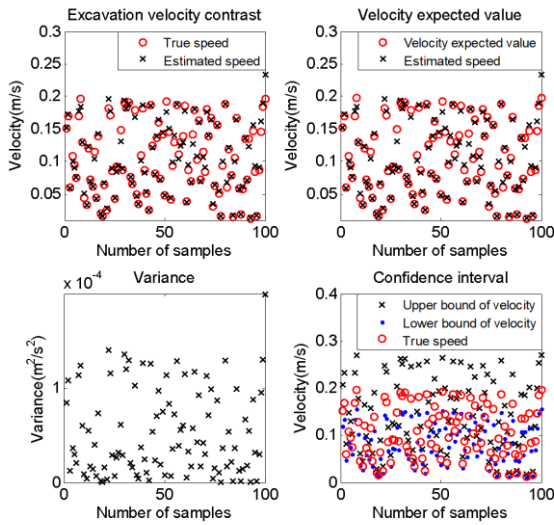
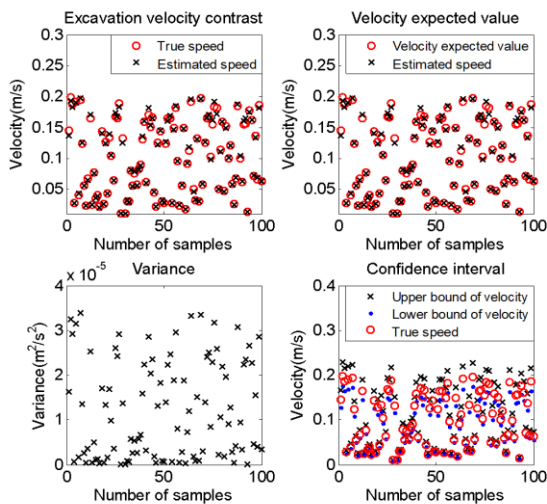**FIGURE 5.** Underground excavation simulation results (D=5 m).

FIGURE 6. Underground excavation simulation results (D=10 m).

FIGURE 7. Underground excavation simulation results (D=15 m).

interval is 95%, the optimal boundary of the velocity estimate is (0.01 m/s∼0.23 m/s), and the estimated speed range is (0.010 m/s∼0.20 m/s).

When the distance between the two ground motion detectors is 15m, the relative deviation range of the excavation speed and the mathematical model for velocity estimation is (0.020%∼4.12%). The relative deviation of the estimated velocity and velocity expectation is (0.060%∼4.08%). The range of variance is (6.83e-7∼0.00020). When the confidence interval is 95%, the optimal boundary of the velocity estimate is (0.010m/s∼0.22m/s), and the estimated speed range is (0.010 m/s∼0.20 m/s).

B. EXPERIMENTAL ANALYSIS
The ground motion detector primarily consists of a moving coil speed sensor and the necessary signal conditioning circuit. Before the experiment, referring to the test standard of seismic exploration instruments, the indexes of the ground motion detector were tested. The test results show that the experimental equipment meets the relevant requirements.

1) SINE WAVE TEST
We use a signal generator as a signal source to output two kinds of sine signals. The frequencies of the sine signals are 30Hz and 50Hz, with a1-V peak-to-peak value. The sampling frequency of the single-chip microcomputer is 610Hz, and the gain is 0dB, as the signal is not amplified. The two sampling curves and their spectral analysis curves in Figures 8 show that the seismic detectors' test frequency and the signal generator's output frequency are the same.

2) CONSISTENCY TEST OF THE SEISMIC DETECTORS
Because multiple seismic detectors are employed in underground excavation systems, each with a separate signal conditioning circuit, it is necessary for the detectors to have good consistency: the acquisition of signals, gain and delay should be consistent. In this paper, two sets of independent seismic detectors were utilized and connected to the power supply.

not large. Table 2 shows the statistics for the data range in Figures 5-7. As shown in Table 2, when the distance between the two ground motion detectors is 5m, the relative deviation range of the excavation speed and the mathematical model for velocity estimation is (0.075%∼16.30%). The relative deviation of the estimated velocity and velocity expectation is (0.015%∼15.90%). The range of variance is (3.35e-7∼0.00015). When the confidence interval is 95%, the optimal boundary of the velocity estimate is (0.0087 m/s∼0.27 m/s), and the estimated speed range is (0.014 m/s∼0.23 m/s).

When the distance between the two ground motion detectors is 10m, the relative deviation range of the excavation speed and the mathematical model for velocity estimation is (0.028%∼7.00%). The relative deviation of the estimated velocity and velocity expectation is (0.0026%∼7.10%).The range of variance is (1.09e-7∼3.20e-5). When the confidence
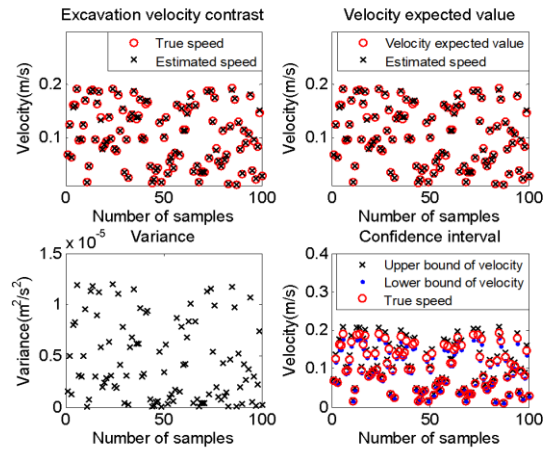
TABLE 3. Test conditions.

The serial number	Working condition
1	Artificial under-ground excavation
2	A person walking

TABLE 4. Main test equipment and tools.

The serial number	Name	Model	Quantity
1	Ground motion detector	ZB-01	2
2	Oscilloscope	Hantek6022BE	1
3	Connecting line	BNC	Several
4	Tape measure		1
5	Laptop		1
6	Battery		4
7	Stopwatch		1
8	Spade		1
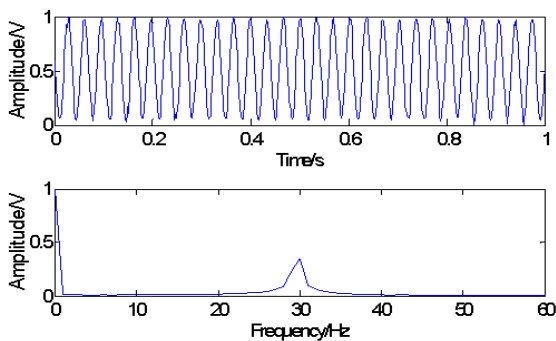
FIGURE 8. Test results for a sine signal at 30 Hz.

FIGURE 10. First 5000 sampling points of the signal for two devices.

The two channels of the oscilloscope are used to collect the seismic signals with a sampling frequency of 1kHz in the indoor test.
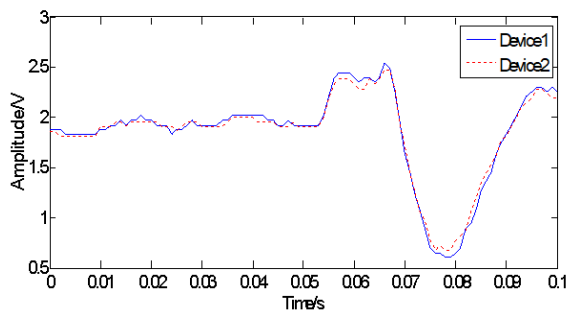

FIGURE 9. First 100 sampling points of the signal for two devices.

The collected waveforms are shown in Figure 9 and Figure 10, and it can be seen that the signal waveforms collected by the two sets of seismic detectors are basically the same.
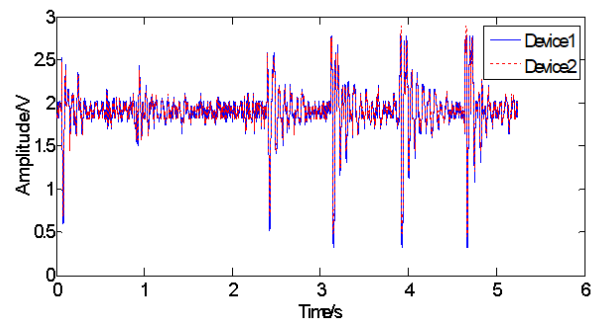
3) TEST CONTENTS AND EQUIPMENT
The ground motion signals caused by personnel under different working conditions are shown in Table 3. A list of the main test equipment and tools is given in Table 4.

4) EXPERIMENTAL PROCEDURE
To satisfy ideal conditions such as geological coincidence, isotropy, ideal elastic medium and so on, this paper uses a site with good geological conditions for testing. According to the field data, a flat grassland was chosen.

The test site is shown in Figure 11, and the target source moved at a certain rate on a predetermined trajectory. For the differences in the seismic signal strength caused by the distance of the target, the target moved as much as possible toward the center of the sensor from far away and nearby. When the target source enters the detection range, the ground motion detector starts to collect data, sending information to the monitoring terminal in real-time through wireless communication. After the acquisition is completed, the collected ground motion signals are processed at the monitoring terminal.

Serial number	Working condition	True speed (m/s)	The calculated speed of the test (m/s)
1	A person walking（D=5m）	1.3m/s	1.5m/s
2	A person walking（D=10m）	1.3m/s	1.3m/s
3	A person walking（D=15m）	1.3m/s	1.3m/s
4	Artificial under-ground excavation（D=5m）	0.2m/s	0.3m/s
5	Artificial under-ground excavation（D=10m）	0.2m/s	0.3m/s
6	Artificial under-ground excavation（D=15m）	0.2m/s	0.2m/s

FIGURE 11. Test site.

After the information measured by the two ground motion detectors is processed, we can see that (as shown in Table 5) when D=5m, the relative deviation between the walking speed measured by the detector and the actual speed is 15%. When D=10m, the relative deviation between the measured walking speed and the actual speed is 0. When D=15m, the relative deviation between the measured walking speed and the actual speed is 0.

After the information measured by the two ground motion detectors is processed, we can see that when D=5 m, the relative deviation between the artificial excavation speed measured by the detector and the actual speed is 50%. When D=10m, the relative deviation between the artificial excavation speed measured by the detector and the actual speed is 50%. When D=15m, the relative deviation between the artificial excavation speed measured by the detector and the actual velocity is 0.

Although the experimental results and theoretical calculation are slightly different, the trend of the theoretical calculation is correct. The main reason for the difference is that the detection accuracy of the ground motion detector is limited, the number of effective digits is small, and there is a certain delay in the test. There are some delays in the synchronization of the two ground motion detectors. These reasons lead to a certain deviation between the simulation analysis and the experimental results.

IV. CONCLUSION

In this paper, a method for estimating velocity based on a two-point synchronization measurement is proposed.

The method uses the simultaneous detection of two seismic detectors to obtain ground motion signals and to estimate the target's velocity. The established target speed estimation model, statistical model, simulation analysis and field experiment show that this method can effectively identify underground mining. This method can be applied to underground excavation monitoring systems that protect military fortifications, enabling defenders to efficiently and accurately determine whether the attacking side is attacking by excavation.

In the future, speed-based information recognition will be combined with an advanced signal processing algorithm and machine learning with the aim of achieving better engineering application results.

REFERENCES

[1] A. M. Zeki, E. E. Elnour, A. A. Ibrahim, C. Haruna, and S. Abdulkareem, "Automatic interactive security monitoring system," in *Proc. Int. Conf. Res. Innov. Inf. Syst. (ICRIIS)*, Nov. 2013, pp. 215–220.

[2] P. Dheenathayalan, M. Caro Cuenca, P. Hoogeboom, and R. F. Hanssen, "Small reflectors for ground motion monitoring with InSAR," *IEEE Trans. Geosci. Remote Sens.*, vol. 55, no. 12, pp. 6703–6712, Dec. 2017.

[3] Y. Li, Z. Q. Wu, J. Q. Li, and X. C. Luo, "Study on traveling wave signal anti-interference and a new detection method," *Appl. Mech. Mater.*, vol. 734, pp. 40–45, Feb. 2015.

[4] J. Bartrand and R. E. Abbott, "Using co-located rotational and translational motion sensors to characterize seismic scattering in the P-wave coda," in *Proc. AGU Fall Meeting*, 2017, p. 691.

[5] A. Mottahedi, F. Sereshki, and M. Ataei, "Overbreak prediction in underground excavations using hybrid ANFIS-PSO model," *Tunnelling Underground Space Technol.*, vol. 80, pp. 1–9, Oct. 2018.

[6] Q. Chen, "Parameters sensitivity analysis of underground excavation impacting on slope stability based on vector sum method," in *Proc. IOP Conf. Ser., Earth Environ. Sci.*, vol. 108, Jan. 2018, Art. no. 032065.

[7] V. Baryshnikov and D. Baryshnikov, "Experimental research data on stress state of salt rock mass around an underground excavation," in *Proc. IOP Conf. Ser., Earth Environ. Sci.*, vol. 134, Mar. 2018, Art. no. 012004.

[8] A. Cantone, R. Fico, F. Cavuoto, and A. Mandolini, "Modelling and monitoring of an urban underground excavation," in *Proc. 11th East Asia–Pacific Conf. Struct. Eng. Construct. (EASEC)*, 2008, pp. 231–238.

[9] A. J. Hoffman, C. Hoogenboezem, N. T. van der Merwe, and C. J. A. Tollig, "Seismic buffer recognition using mutual information for selecting wavelet based features," in *Proc. IEEE Int. Symp. Ind. Electron. (ISIE)*, vol. 2, Jul. 1998, pp. 663–667.

[10] J. H. Mcquiddy, "Advanced unattended sensors and systems: State of the art and future challenges," *Proc. SPIE*, vol. 7693, pp. 76931J-1–76931J-10, May 2010.

[11] S. S. Blackman, "Multiple hypothesis tracking for multiple target tracking," *IEEE Aerosp. Electron. Syst. Mag.*, vol. 19, no. 1, pp. 5–18, Jan. 2004.

[12] A. Pakhomov and E. T. Goldberg, "A novel method for footstep detection with an extremely LowFalse alarm rate," *Proc. SPIE*, vol. 5090, pp. 186–193, Sep. 2003.

[13] A. Subramanian, K. G. Mehrotra, and C. K. Mohan, "Feature selection and occupancy classification using seismic sensors," in *Proc. IEA/AIE*, vol. 6097, 2010, pp. 605–614.

[14] G. Jiawei, L. I. Yongshu, and W. Hongshu, "Information detection of seismic debris flow by UAV high-resolution image based on transfer learning," *Earthq. Res. China*, vol. 33, no. 1, p. 10, 2019.

[15] M. Bagheri and M. A. Riahi, "Seismic facies analysis from well logs based on supervised classification scheme with different machine learning techniques," *Arabian J. Geosci.*, vol. 8, no. 9, pp. 7153–7161, 2015.

[16] A. Pakhomov and T. Goldburt, "Field testing of new unattended small size seismic module for various target detection," *Proc. SPIE*, vol. 6394, Oct. 2006, Art. no. 63940D.

[17] D. Venkatraman, V. V. Reddy, and A. W. H. Khong, "Polarization-cum-energy metric for footstep detection using vector-sensor," in *Proc. IEEE Int. Conf. HST*, Nov. 2011, pp. 196–201.

[18] R. Damarla and D. Ufford, "Personnel detection using ground sensors," *Proc. SPIE*, vol. 6562, May 2007, Art. no. 656205.

[19] A. Pakhomov and T. Goldburt, "Zero false alarm seismic detection and identification systems," *Proc. SPIE*, vol. 6943, Apr. 2008, Art. no. 694317.

[20] S. Schumer, "Analysis of human footsteps utilizing multi-axial seismic fusion," in *Proc. IEEE Int. Conf. Acoust., Speech Signal Process. (ICASSP)*, May 2011, pp. 697–700.
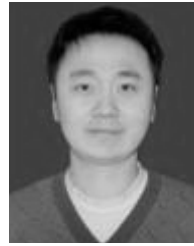
DONGZE QIN received the B.E. degree from the North China Institute of Technology, in 2003, the M.S. degree from the North University of China, in 2006, and Ph.D. degree from the Beijing Institute of Technology, in 2013. Since June 2014, he has been an Associate Professor with the North University of China. His research interests are laser fuzes and signal processing.

JINSHI ZHANG received the bachelor's degree in electrical engineering and intelligent control from the North University of China, in 2017, where he is currently pursuing the master's degree in weapon engineering. His research interests are laser fuzes and signal processing.

● ● ●